Vision Research 50 (2010) 810–817

Contents lists available at ScienceDirect

Vision Research

journal homepage: www.elsevier.com/locate/visres

Arrested development: High-resolution imaging of foveal morphology in albinism

John T. McAllister [a,1], Adam M. Dubis [b,1], Diane M. Tait [a,1], Shawn Ostler [a], Jungtae Rha [a], Kimberly E. Stepien [a], C. Gail Summers [c], Joseph Carroll [a,b,d,*]

[a] Department of Ophthalmology, Medical College of Wisconsin, Milwaukee, WI, USA
[b] Department of Cell Biology, Neurobiology, & Anatomy, Medical College of Wisconsin, Milwaukee, WI, USA
[c] Departments of Ophthalmology and Pediatrics, University of Minnesota, Minneapolis, MN, USA
[d] Department of Biophysics, Medical College of Wisconsin, Milwaukee, WI, USA

ARTICLE INFO

Article history:
Received 9 November 2009
Received in revised form 3 February 2010

Keywords:
Albinism
Cone mosaic
Fovea
Retinal development
Retinal imaging

ABSTRACT

Albinism, an inherited disorder of melanin biosynthesis, disrupts normal retinal development, with foveal hypoplasia as one of the more commonly associated ocular phenotypes. However the cellular integrity of the fovea in albinism is not well understood – there likely exist important anatomical differences that underlie phenotypic variability within the disease and that also may affect responsiveness to therapeutic intervention. Here, using spectral-domain optical coherence tomography (SD-OCT) and adaptive optics (AO) retinal imaging, we obtained high-resolution images of the foveal region in six individuals with albinism. We provide a quantitative analysis of cone density and outer segment elongation demonstrating that foveal cone specialization is variable in albinism. In addition, our data reveal a continuum of foveal pit morphology, roughly aligning with schematics of normal foveal development based on post-mortem analyses. Different albinism subtypes, genetic mutations, and constitutional pigment background likely play a role in determining the degree of foveal maturation.

1. Introduction

Albinism is an inherited disorder of melanin biosynthesis, associated with absent or reduced melanin pigment in the eye, and often in the skin and hair. Oculocutaneous albinism type 1 (OCA1; MIM 203100) is a recessive disorder in which individuals have a mutation in the tyrosinase gene on chromosome 11q14.3. Those who never develop any melanin pigment within the eye, hair, and skin have OCA1A, while those with development of some melanin pigment due to a "leaky" mutation that allows residual enzyme activity have OCA1B (King et al., 2003). Ocular albinism (OA1; MIM 300500) is characterized by X-linked inheritance and has been mapped to Xp22.3–Xp22.2. The affected males typically have normal skin and hair pigment, but will usually have all the ocular-visual manifestations of albinism, including iris transillumination, macular translucency, photosensitivity, refractive errors, astigmatism, nystagmus, impaired stereopsis, altered retinostriate decussation, and reduced visual acuity (Oetting, Summers, & King, 1994; Summers, 2009).

The normal human fovea underlies the majority of our visual function, including color vision and high spatial acuity vision, and is characterized by an avascular zone, an increase in cone photoreceptor density, and an excavation of inner retinal neurons (Hendrickson, 2005). Foveal manifestations of albinism can include absence of a foveal avascular zone (Abadi & Pascal, 1989; Gregor, 1978), foveal hypoplasia (absence of a foveal pit) (Kinnear, Jay, & Witkop, 1985; Oetting et al., 1994), and loss of an annular reflex (Lee, King, & Summers, 2001). Reductions in visual acuity have been attributed to absent melanin synthesis and the absence of a foveal pit (Seo et al., 2007), however certain patients with some melanin pigment in their maculae due to residual enzyme activity still show decreased visual acuity and others with poorly defined foveal pits have relatively preserved visual acuity (Harvey, King, & Summers, 2006; Summers, 1996). As such, significant work remains in elucidating the relationship between foveal maldevelopment and visual function in albinism (Jeffery, 1997). This lack of clarity stems in part from ambiguity surrounding foveal anatomy in albinism, specifically with regard to foveal cone specialization.

There are but a few cases in the literature that deal directly with the issue of cone specialization in human albinism, and they are far from unified in their findings. In a post-mortem analysis, Fulton, Albert, and Craft (1978) found that central cone density in a patient

Abbreviations: AO, adaptive optics; ELM, external limiting membrane; IS, inner segment; ILM, internal limiting membrane; OA, ocular albinism; OCA, oculocutaneous albinism; OCT, optical coherence tomography; ONL, outer nuclear layer; OPL, outer plexiform layer; OS, outer segment; RPE, retinal pigment epithelium.

* Corresponding author. Address: Medical College of Wisconsin, The Eye Institute, 925 N. 87th Street, Milwaukee, WI 53226, USA. Fax: +1 414 456 6690.
E-mail address: jcarroll@mcw.edu (J. Carroll).

[1] These authors contributed equally to this work.

0042-6989/$ - see front matter © 2010 Elsevier Ltd. All rights reserved.
doi:10.1016/j.visres.2010.02.003

with OCA was significantly *decreased* compared to values normally found in the parafoveal region (Fulton et al., 1978). In another histological study on an OCA retina, *increased* cone density was observed in the fovea compared to the periphery, though it was not reported whether the foveal density was consistent with normal values (Akeo et al., 1996). Wilson, Mets, Nagy, and Kressel (1988) measured grating acuity in two OCA patients and found a defect in spatial processing in the central retina that was best explained by an increased spacing of the central cone photoreceptors. Based on multifocal electroretinogram findings, it has been inferred that the density of cone photoreceptors across the central retina is homogeneous in OCA (Kelly & Weiss, 2006) and in ocular albinism (OA) (Nusinowitz & Sarraf, 2008), consistent with an underdeveloped macular region.

Recent advances in high-resolution imaging make it possible to quantitatively assess foveal morphology in the living retina. Optical coherence tomography (OCT) offers high axial resolution and enables visualization of retinal lamination, while adaptive optics (AO) provides high lateral resolution and allows direct visualization of the cone photoreceptor mosaic. Here we applied these imaging tools to characterize the foveal cone specialization in four individuals with OCA1B and two with OA1. We observed varying degrees of foveal maturity and cone specialization in the albinotic retina, which roughly align with schematics of normal foveal development based on post-mortem analyses (Isenberg, 1986; Mann, 1950; Provis, Diaz, & Dreher, 1998; Springer, 1999). This supports the idea that, in general, normal foveal development is arrested in individuals with albinism (Wilson et al., 1988). As such, examining foveal morphology and cone specialization in albinism may offer valuable insight into the process of normal foveal development. In addition, as previous work suggests that it may be possible to recover some aspect of foveal maturity in albinism through L-DOPA supplementation (Ilia & Jeffery, 1999, 2000; Lopez, Decatur, Stamer, Lynch, & McKay, 2008; Reis, Ventura, Kubrusly, de Mello, & de Mello, 2007), better, more quantitative measures of foveal architecture in albinism are needed. The tools described here should prove useful for dissecting retinal versus cortical roles in vision loss in albinism, evaluating therapeutic strategies for albinism, and for more accurately characterizing post-natal foveal development in the normal retina.

2. Methods

2.1. Human subjects

This study adhered to the tenets of the Declaration of Helsinki and was approved by the Children's Hospital of Wisconsin Institutional Review Board. Participants provided written informed consent after explanation of the nature and possible consequences of the study. Two subjects with X-linked OA1 (both male), four with OCA1B (three male and one female), and 167 control subjects without albinism (72 males, 95 females with a mean age of 32.6) were recruited for retinal imaging. The control subjects excluded individuals with color vision deficiency or history of ocular surgery or other diagnosed retinal abnormalities. Fundus photographs were obtained from the subjects with albinism and were evaluated for fundus pigmentation, foveal reflex, foveal vasculature, and general anatomical features. These photos, in addition to clinical examination, were used to classify each of the subjects with albinism by phenotype. A summary of clinical characteristics can be found in Table 1.

2.2. Spectral-domain optical coherence tomography (SD-OCT)

Volumetric images of the macula were acquired using the Zeiss Cirrus HD-OCT (Carl Zeiss, Meditec, Dublin CA, USA). Volumes were 6 mm × 6 mm and consisted of 128 B-scans (512 A-scans/B-scan). At least three replicate scans were acquired to assess repeatability of fixation and allow an estimation of the preferred retinal locus of fixation. For each subject with albinism, images containing a Cirrus LSO (laser scanning ophthalmoscope) map, retinal thickness map, and volume scan boundaries were extracted and registered to a color fundus image using i2k Align Retina software (DualAlign, LLC, Clifton Park, NY USA). The LSO images with OCT boundaries contain a cross hair depicting the center of the scan, which by design, corresponds to fixation for that particular volume scan. After all replicate Cirrus LSO maps were registered to the color fundus image, the center of fixation was identified for each image, and their absolute positions within the fundus recorded. The center of mass of these locations was calculated to derive a single estimate of the preferred retinal locus of fixation. In addition, the position of the center of the retinal doming was approximated, and its position within the fundus recorded for each subject. The expected location of the fovea was also calculated based on data from Rohrschneider (2004). Some subjects had cyclotropia, and their photos were corrected prior to calculation of the expected foveal location (Bixenman & Von Noorden, 1982). In all cases, the locus of fixation was close to the expected foveal location, however errors in this calculation could affect our absolute topographical analysis of cone density.

High-resolution SD-OCT (Bioptigen, Inc., Durham, NC) imaging was performed in all six subjects with albinism and the 167 controls. Line scan sets were acquired (1000 A-scans/B-scan; 100 repeated B-scans) through the center of the foveal center (either the actual fovea or expected foveal location when there was no visible pit). Scans were registered and averaged as previously described to reduce speckle noise in the image (Tanna et al., 2009).

The inner limiting membrane (*ILM*), external limiting membrane (*ELM*), inner segment-outer segment junction (*IS/OS*), and two layers representing the retinal pigment epithelium (*RPE1, RPE2*) were manually segmented. Demarcated retinal layers were then interpolated and layer thicknesses were extracted using programs developed with Matlab™ (Mathworks, Natick, MA). The distance between the ILM and RPE2 provided total retinal thickness, the distance between the center of the ELM and center of the IS/OS junction provided inner segment (IS) thickness, while the distance between the center of the IS/OS and center of RPE1 provided the outer segment layer (OS) thickness. The scan length of each OCT scan set was corrected for inter-individual differences in axial length based on Bennett, Rudnicka, and Edgar (1994). Interpolated thickness values for each subjects' IS and OS layer were binned and averaged at 0.1 mm incre-

Table 1
Clinical summary of subjects with albinism.

Subject	Sex	Age	Diagnosis	Foveal pit (on OCT)	Visual acuity (BCVA)	Axial length (OD)	Axial length (OS)	Nystagmus
JC103	M	16	OA1	None	20/70	22.58	22.37	Horizontal pendular
JC0125	M	27	OCA1B	None	20/60+	22.49	22.08	Horizontal pendular
AD0063	M	32	OA1	None	20/40	24.16	26.97	None
JC0140	M	10	OCA1B	Indistinct	20/20−3	22.06	22.08	None
JC0170	F	16	OCA1B	Indistinct	20/40	23.84	23.62	Horizontal pendular
JC0131	M	20	OCA1B	Indistinct	20/40+	24.94	24.87	Horizontal pendular

ments between 2 mm nasal and 2 mm temporal retina. The relative foveal lengthening of the IS (or OS) layer was computed by dividing the foveal IS (or OS) thickness by the average IS (or OS) thickness at 1.75 mm nasal and temporal to the fovea.

2.3. Adaptive optics (AO) imaging

An AO fundus camera was used to acquire images of the cone mosaic. The subjects' eye was dilated and accommodation suspended using one drop each of phenylephrine hydrochloride (2.5%) and tropicamide (1%). The AO system housed at the Medical College of Wisconsin has been described in detail elsewhere (Rha, Schroeder, Godara, & Carroll, 2009), a brief summary of the system is given here. The eye's monochromatic aberrations are compensated for using a 52-channel deformable mirror (Imagine Eyes, Orsay, France). Retinal images are acquired by illuminating the retina with a 1.8-deg diameter, 500 ms flash from a fiber-coupled near infrared source ($\lambda = 837.8$ nm; $\Delta\lambda = 14.1$ nm). To reduce speckle noise in the image the spatial coherence of the laser was reduced by using 110 m of multimode step index fiber (Fiberguide Industries, Stirling, NJ, USA). A back-illuminated scientific-grade 12-bit charge-coupled device, the Cam1M100-SFT (Sarnoff Corporation, Princeton, NJ), captured images of the retina. During each 500 ms flash, continuous images of the retina are collected at a frame rate of 167 fps with 6 ms exposure. Individual frames are registered then averaged using a MatLab-based algorithm (MathWorks, Natick, MA) for subsequent analysis.

Individual cones in each image were identified using a semi-automated cone identification program based on the work of Li and Roorda (2007). As the results of this algorithm depend on the spatial filter applied to the image, we added an objective procedure for setting this filter. The user selected a group of cones manually, and the mean nearest neighbor distance of these cones was used to set the spatial filter. The filtered image was then fed through the automated algorithm to identify individual cones. From this data cone density (cones/mm^2) was calculated as previously described (Carroll, Neitz, Hofer, Neitz, & Williams, 2004). Regularity of the cone mosaic was assessed using a previously described Voronoi analysis (Baraas et al., 2007). In all cases, the approximate retinal location of the cone mosaic images relative to the incipient foveal center was determined based on the fundus images using common blood vessel patterns and that subjects' suspected locus of fixation.

3. Results

3.1. Gross assessment of foveal morphology in albinism

To qualitatively assess gross foveal topography, we acquired both cross-sectional and volumetric images of the central macula using SD-OCT (Fig. 1). The high-resolution foveal cross sections from the Bioptigen SD-OCT system (Fig. 1, panels A–F) and the macular thickness maps obtained from Cirrus HD-OCT volumes (Fig. 1, panels I–N) reveal a continuum of foveal maturity across the albinotic subjects. Some individuals have nearly planar thickness across the macula (Fig. 1, panels A, B, I, J), one has marked doming in his retinal thickness (Fig. 1, panels C and K), and the others have a shallow foveal depression and some excavation of inner retinal neurons in a region of increased retinal thickness (Fig. 1, panels D–F and L–N). The "doming" of the macular region is thought to precede the formation of a fovea centralis (Provis et al., 1998; Springer, 1999). The two normals (Fig. 1, panels G, H and O, P) represent the minimum and maximum foveal pit depth observed in the 167 normal controls in this study and illustrate the degree of variation in normal foveal pit morphology (Dubis, McAllister, & Carroll, 2009). Among those subjects with albinism without a pit, there was no discernable lengthening of the photoreceptor OS at the fovea whereas among those with a rudimentary pit and the normal subjects, there was visible lengthening of the photoreceptor OS in the central fovea.

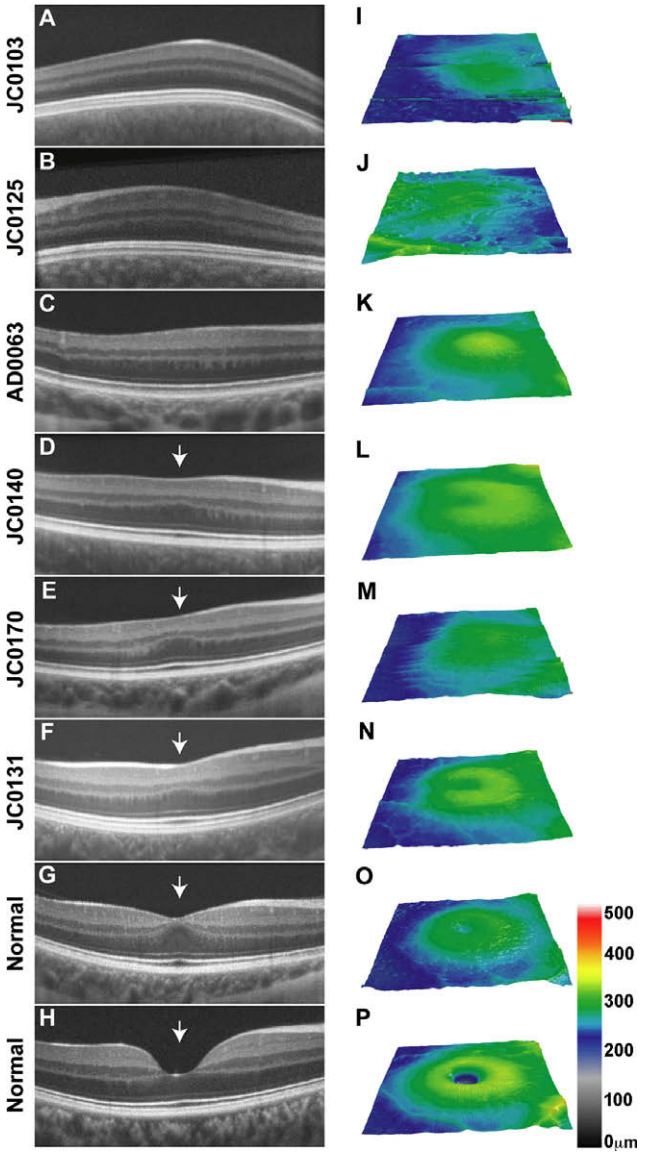

Fig. 1. SD-OCT imaging of foveal morphology. (A–H) Linear SD-OCT scans through the central macula in six albinotic subjects (A–F) and two normal controls (G,H). Arrows mark the center of the foveal pit, when present. (I–P) Retinal thickness maps for the six albinotic subjects (I–N) and two normal controls (O,P). All scans are right eye except subject JC0125 (B,J), which is left eye.

3.2. Quantifying foveal cone specialization using SD-OCT

As the fovea develops, the IS and OS of the foveal cones become longer, and this process is thought to continue as long as 4 years after birth (Yuodelis & Hendrickson, 1986). As a metric of foveal cone specialization, we developed a quantitative approach to assess IS and OS maturation based on the high-resolution SD-OCT images. Shown in Fig. 2 are images from one of the normal controls, specifying the identity of the different layers in the parafoveal (Fig. 2A) and foveal regions (Fig. 2B) on an SD-OCT scan. The IS can be clearly demarcated on the OCT scans as the distance between the ELM & IS/OS junction, while the OS length is given by the distance between the IS/OS junction and the OS/RPE interface (RPE1). We mapped the IS and OS pho-

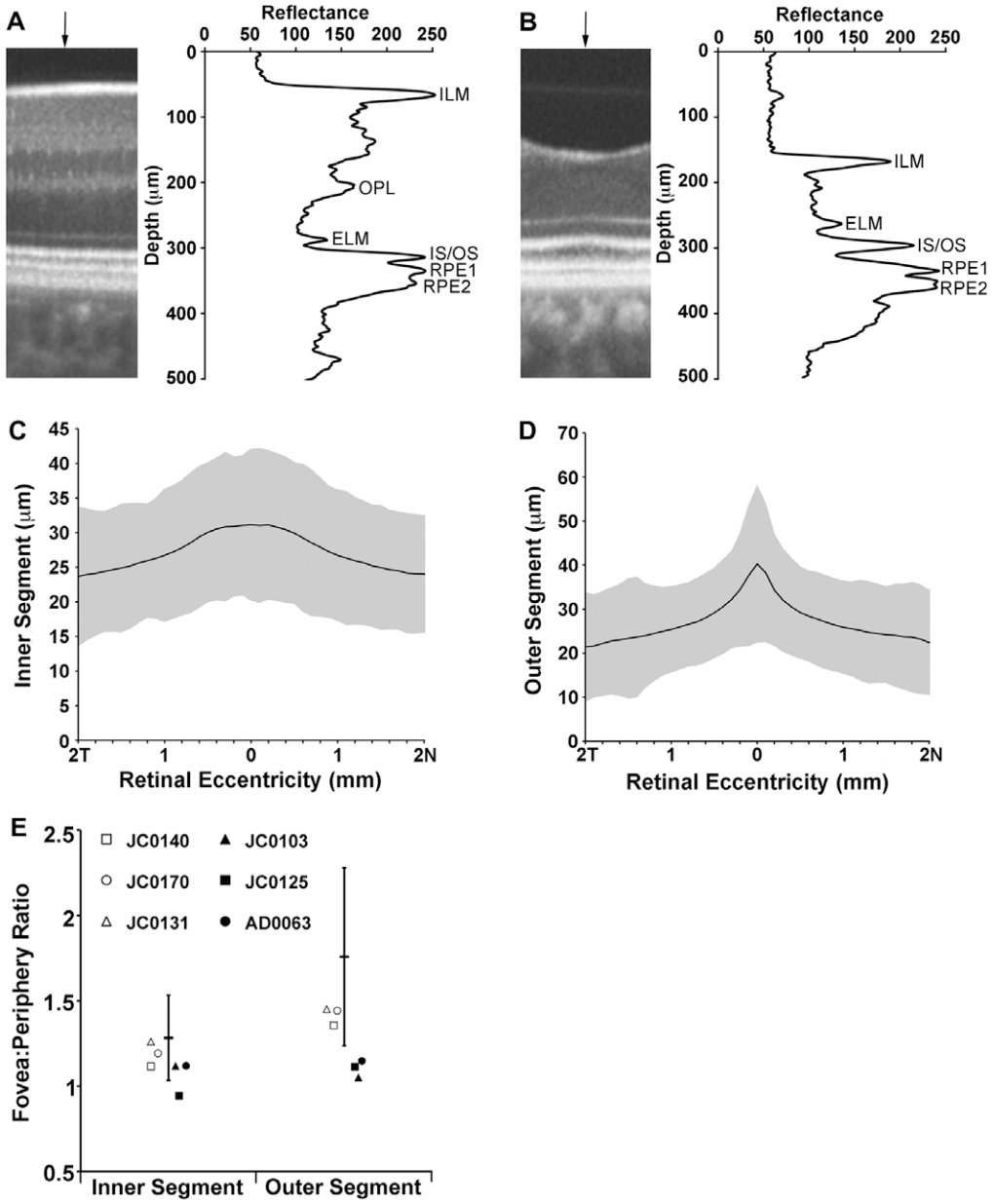

Fig. 2. Quantifying cone photoreceptor dimensions with SD-OCT. (A) SD-OCT image at approximately 1.75 mm temporal from the fovea in a normal retina. (B) SD-OCT image near the foveal center in the same retina. Line plots in A and B represent an average of three longitudinal reflectivity profiles (LRP) through the corresponding SD-OCT image at the location of the vertical arrows above each SD-OCT scan. ILM = inner limiting membrane; OPL = outer plexiform layer; ELM = external limiting membrane; IS/OS = inner segment/outer segment junction; RPE1 = outer segment/retinal pigment epithelium interface; RPE2 = retinal pigment epithelium/Bruch's membrane. (C) Plot of normal IS thickness (black line) as a function of retinal location along the horizontal meridian. (D) Plot of normal OS thickness (black line) as a function of retinal location along the horizontal meridian. Shaded gray region in C and D is ±2 SD for the 167 normal controls. (E) Ratio of foveal:peripheral IS and OS lengths. Foveal value taken as the IS (or OS) length at the center of the foveal pit. In the three albinotic retinas with no visible pit, the foveal value was taken at the location of the maximum doming. Peripheral value is an average of the IS (or OS) thickness at 1.75 mm nasal and temporal to the foveal location. The normal mean IS and OS ratios are plotted as horizontal bars, with the error bars representing ±2 SD. Filled symbols represent the IS and OS ratios for the individuals deemed to have no obvious foveal pit on SD-OCT, while open symbols represent ratios for those individuals with a rudimentary pit present on SD-OCT. All but one subject (JC0103) had IS ratios within 2SD of the normal mean, where as only the individuals with visible pits had OS ratios within 2SD of the normal mean.

toreceptor lengths along the horizontal meridian for the 167 normal subjects and found a pronounced lengthening of the OS layer in the fovea relative to that in the parafovea (Fig. 2C). There was a slight increase in IS length in the fovea compared to that in the parafovea (Fig. 2D). At the fovea, the IS are 1.34 times longer than in the periphery while the OS are 1.87 times longer in our normal subjects (Fig. 2E). This lengthening is a well-described feature of the adult retina (Yuodelis & Hendrickson, 1986) and the magnitude of the lengthening observed here *in vivo* is consistent with that reported from histology (Hoang, Linsenmeier, Chung, & Curcio, 2002). The subjects with albinism without a visible pit on SD-OCT had minimal to no foveal lengthening of the IS and OS whereas the individuals with a rudimentary pit had IS and OS lengthening that was within the normal range.

3.3. Quantifying foveal cone specialization using adaptive optics imaging

During foveal development there is also significant central migration of the cone photoreceptors, resulting in a decrease in

their diameter and an increase in packing density (Diaz-Araya & Provis, 1992; Yuodelis & Hendrickson, 1986). We examined this by imaging the cone photoreceptor mosaic using an adaptive optics fundus camera. Images of the cone mosaic from 1-deg superior retina from a normal control (Fig. 3A) and two of the subjects are shown (Fig. 3B and C). An image from a subject with OCA1B (Fig. 3B) reveals a gradual decrease in cone packing density moving from left (inferior retina) to right (superior retina). A corresponding image from a subject with OA1 (Fig. 3C) reveals more uniform cone packing density. Colored strips below each image are Voronoi diagrams from the center of the corresponding image, which allows easier visualization of cone packing. The gradual decrease in cone packing for the normal control (Fig. 3A) and OCA1B subject (Fig. 3B) can be seen as an increase in the area of the Voronoi polygons, whereas the image from the OA1 subject (Fig. 3C) has more uniformly-sized polygons. We measured the percentage of cones with six-sided (green) Voronoi domains as a metric of regularity (Baraas et al., 2007; Li & Roorda, 2007; Pum, Ahnelt, & Grasl, 1990) and found that the normal subject had 57% (Fig. 3A), the OCA1B subject had 53% (Fig. 3B), and the OA1 subject had 53% (Fig. 3C). These are consistent with previously published values for the normal retina at this eccentricity (Baraas et al., 2007; Li & Roorda, 2007). Cone density values for all subjects are shown in Fig. 3E, and there is variation in the degree of cone packing moving towards the fovea. Importantly, in two of the patients shown not to have significant OS lengthening (JC0125, AD0063), there was a progressive increase in cone packing toward the fovea. This appears to be consistent with earlier data that cone packing and OS lengthening are decoupled events, specifically that cone IS reach adult diameters before cone OS reach adult lengths (Yuodelis & Hendrickson, 1986). These measurements provide yet another level of resolution for quantifying foveal maturity with *in vivo* retinal imaging.

3.4. Visualizing pigment mottling in the albinotic retina

In one of the subjects with albinism (JC0140), we were able to visualize melanin pigment clumping throughout the central fovea (Fig. 4A–E). Pigment clumping was observed in the fundus photograph (see Supplementary Fig. S1). While in the normal retina there are intraretinal variations in cone reflectivity (Pallikaris, Williams, & Hofer, 2003) and low frequency undulations in image intensity across adaptive optics images of the cone mosaic (Fig. 4F), this individual had discrete patches of hypo- and hyper-reflective retina. We posit that the hyper-reflective areas contain little or no melanin resulting in increased light scatter, while the hypo-reflective areas represent the melanin clumping. Interestingly, the cones within the brighter patches are variable in reflec-

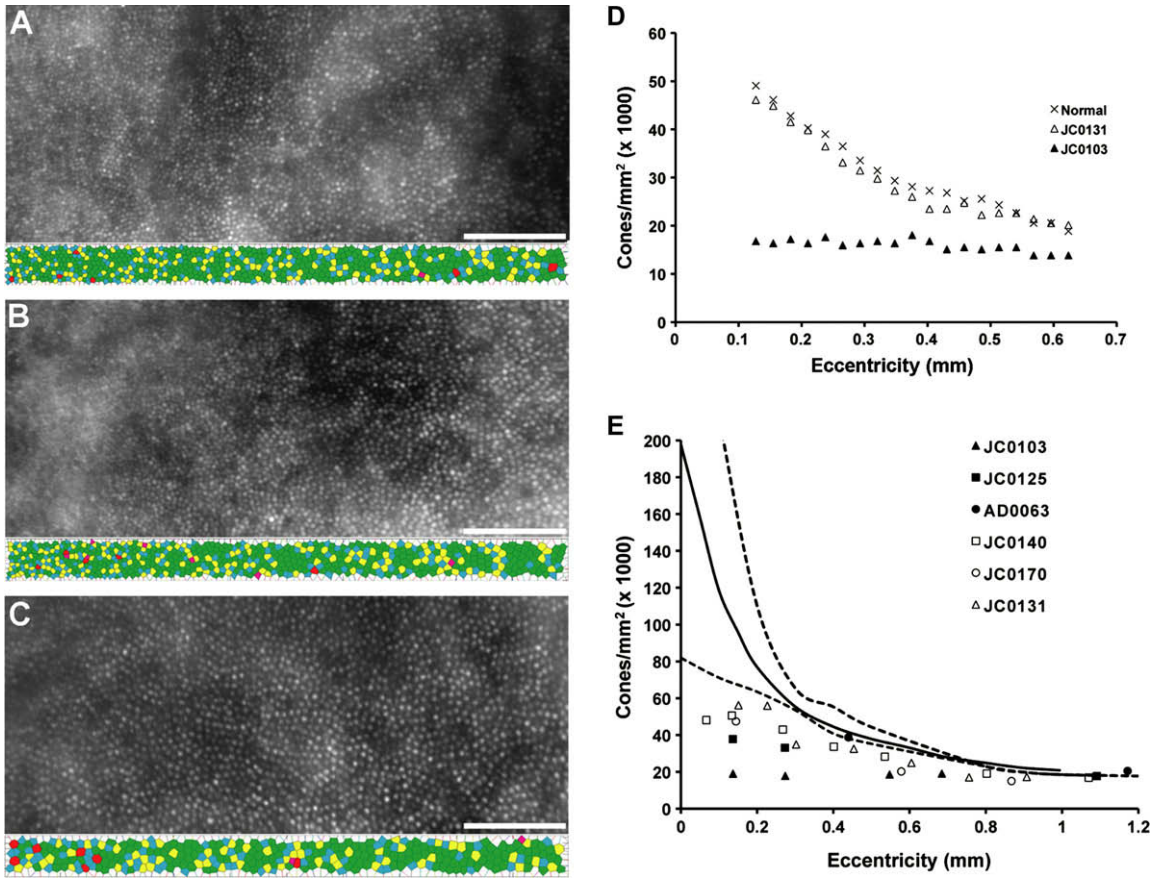

Fig. 3. Variability in cone packing in albinism. Shown are images of the cone mosaic centered at approximately 1 deg superior retina. The foveal center is located just off the left edge of each image. Images from a normal retina (A) and a subject with OCA1B (B) reveal a gradual decrease in cone packing density moving from left (inferior retina) to right (superior retina). Corresponding image from a subject with OA1 (C) reveals more uniform cone packing density. Scale bar is 100 μm. Color panels in A–C are Voronoi diagrams of a central strip through each image. Green color indicates Voronoi domains with six sides, reflecting the hexagonal packing of the cone mosaic. Other colors indicate domains with fewer or greater than six sides. The gradual decrease in cone packing (A and B) can be seen in the Voronoi diagrams as an increase in the area of the polygons, whereas the image in C has more uniformly-sized polygons. (D), Plot of cone density as a function of retinal location for the mosaics in A–C. (E), Cone density as a function of retinal eccentricity. Filled symbols represent cone density values for albinism patients deemed to have no obvious foveal pit on SD-OCT, while open symbols represent densities for those individuals with a rudimentary pit present on SD-OCT. Only one subject (JC0103) showed a uniform density, the remaining subjects showed some degree of cone packing. Solid black and dashed gray lines represent the mean and minimum/maximum, respectively, of previously published normative data from histology (Curcio, Sloan, Kalina, & Hendrickson, 1990).

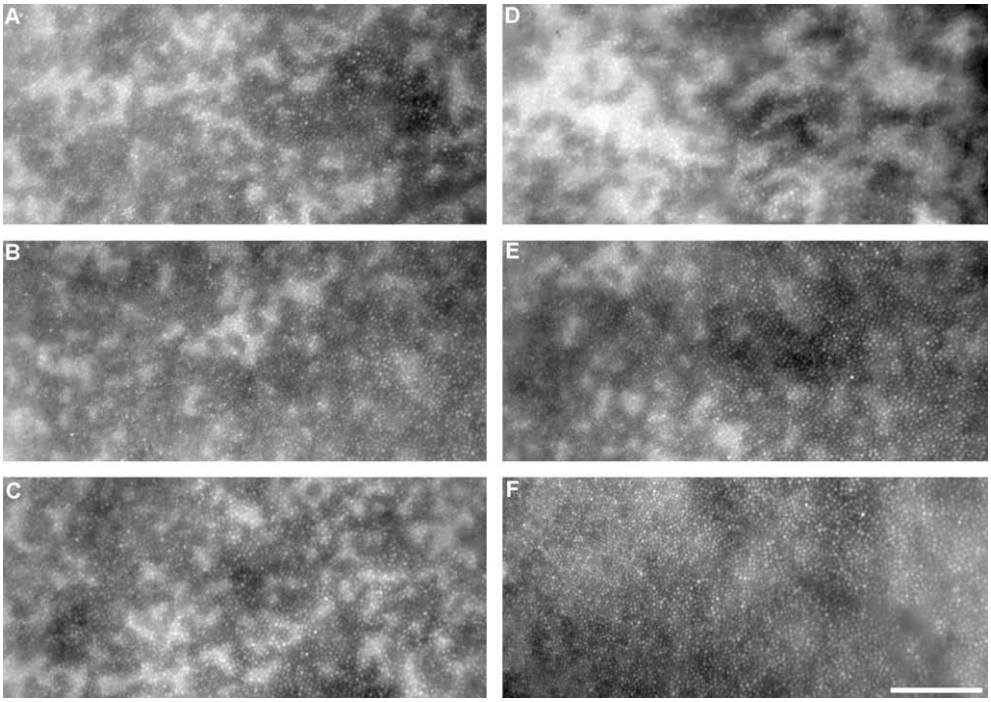

Fig. 4. Visualizing melanin pigment clumping. (A–E) Images of the cone mosaic from a subject with OCA1B (JC0140). While a contiguous cone mosaic is clearly visible throughout the images, the images have a mottled appearance. (F) Images of the cone mosaic from a normal control. Cones vary individually in their reflectivity, and there are regional differences in image intensity, but this is in stark contrast to the mottling seen in A–E. Scale bar is 100 μm.

tivity, just as those within the darker areas are, suggesting that melanin distribution may not be the primary determinant to individual variation in cone reflectivity in AO images. It would be interesting to monitor how these pigmentary clumps change over time in this individual, as well as to examine other individuals with disruptions in melanin biosynthesis and distribution (such as Menkes disease, Wilson disease, Usher Syndrome type 1B, Hermansky-Pudlak syndrome; see King, Oetting, Summers, Creel, and Hearing (2007) for a review) for possible retinal manifestations that may not have been previously recognized.

4. Discussion

Our anatomic data obtained with AO and SD-OCT reflect the lack of consensus regarding the albinotic fovea in the literature. We have shown that foveal specialization can be measured *in vivo* on multiple levels – from morphology of the foveal pit to the length of the cone outer segment. We observed varying degrees of foveal maturity and cone specialization in the albinotic retina, which roughly align with schematics of normal foveal development based on post-mortem analyses (Isenberg, 1986; Mann, 1950; Provis et al., 1998; Springer, 1999). Thus we conclude that there is not a single picture that captures foveal morphology in albinism; rather there is a continuum of foveal maturity associated with the condition. This is likely based on a number of factors, including albinism subtype (OA versus OCA), the specific genetic mutation, and the natural pigment background of the patient. At first glance, the retinas from subjects with OCA1B tended to be more mature than those from the OA1 subjects. However no genetic analysis was done for this study, so more work needs to be done to determine the exact nature of any genotype–phenotype correlation within or across classifications of albinism.

Contrary to a recent report (Marmor, Choi, Zawadzki, & Werner, 2008), none of our subjects with albinism had complete foveal cone specialization. This discrepancy may have to do with examining different albinism subtypes, though Marmor et al. did not provide any quantitative analysis so it is difficult to compare their results with our data. However, our data do support the idea that significant foveal cone specialization can occur in the absence of a foveal pit. In addition, Hendrickson, Djajadi, Erickson & Possin (2006) found that in anencephaly, foveal cone specialization (cone packing and elongation) occurred in the absence of a fully formed foveal pit. These data conflict with the "passive" model of foveal development, which predicts that in the absence of a foveal pit centripetal cone packing would not occur (Hendrickson, Troilo, Possin & Springer, 2006; Springer, 1999; Springer & Hendrickson, 2004a, 2004b, 2005).

A *qualitative* nomenclature is often used to describe the fovea in albinism and related conditions. Foveal hypoplasia literally refers to the absence of a pit, however it has been suggested that the negative functional connotations that accompany this term are reason for a different classification – fovea plana (Marmor et al., 2008). In light of our data, it is clear that neither of these qualitative terms universally applies to albinism and are inadequate descriptors to capture even the purely anatomical phenotype associated with albinism or other disorders where foveal pit morphology is compromised. Thus, we propose that a more *quantitative* description of the central retina be adopted, given the emerging availability of non-invasive high-resolution imaging tools. This is especially relevant given the significant variability observed among the albinotic fovea (Chong et al., 2009; Harvey et al., 2006; Seo et al., 2007); foveal pit maturity and cone specialization are not all-or-none phenomena.

What limits vision in the albinotic visual system? For one, the abnormal retino-cortical projections in albinism (Guillery, Okoro, & Witkop, 1975) presumably compromise stereo vision, though both the degree of chiasmal misrouting (Hoffmann, Tolhurst, Moore, & Morland, 2003; von dem Hagen, Houston, Hoffmann, & Morland, 2007) and reduction in stereo acuity (Lee et al., 2001) are variable. With regard to spatial vision, Wilson et al. (1988) proposed that "*the deficits in central monocular spatial vision of albinos result from the increased spacing and (to a lesser extent) the decreased*

outer segment length of their central cones related to those of normal young adults." This is supported by the finding that reduced cortical volume in a region of the brain that corresponds to the cortical representation of the central retina has been observed in albinism (von dem Hagen, Houston, Hoffman, Jeffery, & Morland, 2005), presumably due to a reduced number of foveally-driven retinal ganglion cells. As we only recorded clinical acuity, it is difficult to draw any conclusions in our patients, however the ability to characterize cone density and OS length *in vivo* should enable further examination of this issue when paired with improved measures of acuity and contrast sensitivity.

In animal studies, it has been shown that the degree of retinal pigmentation is related to the extent of chiasmal misrouting (LaVail, Nixon, & Sidman, 1978; Sanderson, Guillery, & Shackleford, 1974), with lower pigmentation levels being associated with a greater shift in the line of decussation into temporal retina. This was recently also shown to be true in humans with albinism (von dem Hagen et al., 2007), and the authors proposed that if pigmentation were to determine both the extent of foveal hypoplasia and misrouting, then a correlation between acuity and misrouting would be predicted (von dem Hagen et al., 2007). In addition, the level of ocular pigmentation has been shown to affect the clinical features of albinism (Dorey, Neveu, Burton, Sloper, & Holder, 2003; Lee et al., 2001). Such a correlation might help explain differences in vision across albinism subtypes, though further investigation is required. There is a strong relationship between foveal abnormalities and cortical disruption, given recent findings in albinism from MRI, fMRI, and VEP studies (Dorey et al., 2003; Neveu, Von Dem Hagen, Morland, & Jeffery, 2008; von dem Hagen et al., 2005, 2007). However a deficiency of these studies is that no accompanying measures of foveal maturity or cone specialization were made. With the large degree of variation in cone specialization observed in our patients with albinism, it would be interesting to revisit these cortical studies in patients for whom the foveal architecture has been quantified in order to develop a more comprehensive model of reduced visual function in albinism.

Given that foveal development continues after birth, it should soon be possible to visualize with high temporal resolution the progression of the latter stages of foveal development in humans with some of the imaging modalities used here. In particular, handheld SD-OCT technology is now commercially available and has been used to image the infant retina under anesthesia (Chong et al., 2009; Scott, Farsiu, Enyedi, Wallace, & Toth, 2009) and also in the awake state (Chavala et al., 2009; Maldonado et al., 2010). As future treatments aimed at increasing melanin pigment production are likely to be more successful when applied earlier in development, such technology will be required to identify the most favorable candidates and to assess treatment response in these young retinas.

Acknowledgments

J.C. is the recipient of a Career Development Award from Research to Prevent Blindness. This study was supported by NIH Grants P30EY001931, T32EY014537, Fight for Sight, The E. Matilda Ziegler Foundation for the Blind, RD and Linda Peters Foundation, The Gene and Ruth Posner Foundation, Hope for Vision, unrestricted departmental grants to the Medical College of Wisconsin and University of Minnesota from Research to Prevent Blindness, and the Albinism & Related Disorders Research Fund at the Minnesota Medical Foundation. The authors thank Dr. Alfredo Dubra for sharing image registration software, Dr. Pooja Godara, Brett Schroeder, & Phyllis Summerfelt for assistance with retinal imaging, and Dr. Janice Burke, Dr. Thomas Connor, Jr., & Melissa Wagner-Schuman for helpful discussions. The authors thank the patients and their families for their time and assistance with the study.

Appendix A. Supplementary material

Supplementary data associated with this article can be found, in the online version, at doi:10.1016/j.visres.2010.02.003.

References

Abadi, R. V., & Pascal, D. (1989). The recognition and management of albinism. *Ophthalmic & Physiological Optics, 9*, 3–15.

Akeo, K., Shirai, S., Okisaka, S., Shimizu, H., Miyata, H., Kikuchi, A., et al. (1996). Histology of fetal eyes with oculotaneous albinism. *Archives of Ophthalmology, 114*, 613–616.

Baraas, R. C., Carroll, J., Gunther, K. L., Chung, M., Williams, D. R., Foster, D. H., et al. (2007). Adaptive optics retinal imaging reveals S-cone dystrophy in tritan color-vision deficiency. *Journal of the Optical Society of America A, 24*(5), 1438–1446.

Bennett, A. G., Rudnicka, A. R., & Edgar, D. F. (1994). Improvements on Littmann's method of determining the size of retinal features by fundus photography. *Graefe's Archive for Clinical and Experimental Ophthalmology, 232*, 361–367.

Bixenman, W. W., & Von Noorden, G. K. (1982). Apparent foveal displacement in normal subjects and in cyclotropia. *Ophthalmology, 89*, 58–62.

Carroll, J., Neitz, M., Hofer, H., Neitz, J., & Williams, D. R. (2004). Functional photoreceptor loss revealed with adaptive optics: An alternate cause for color blindness. *Proceedings of the National Academy of Sciences USA, 101*(22), 8461–8466.

Chavala, S. H., Farsiu, S., Maldonado, R., Wallace, D. K., Freedman, S. F., & Toth, C. A. (2009). Insights into advanced retinopathy of prematurity using handheld spectral domain optical coherence tomography imaging. *Ophthalmology, 116*, 2448–2456.

Chong, G. T., Farsiu, S., Freedman, S. F., Sarin, N., Koreishi, A. F., Izatt, J. A., et al. (2009). Abnormal foveal morphology in ocular albinism imaged with spectral-domain optical coherence tomography. *Archives of Ophthalmology, 127*(1), 37–44.

Curcio, C. A., Sloan, K. R., Kalina, R. E., & Hendrickson, A. E. (1990). Human photoreceptor topography. *The Journal of Comparative Neurology, 292*, 497–523.

Diaz-Araya, C., & Provis, J. M. (1992). Evidence of photoreceptor migration during early foveal development: A quantitative analysis of human fetal retinae. *Visual Neuroscience, 8*(6), 505–514.

Dorey, S. E., Neveu, M. M., Burton, L. C., Sloper, J. J., & Holder, G. E. (2003). The clinical features of albinism and their correlation with visual evoked potentials. *British Journal of Ophthalmology, 87*(6), 767–772.

Dubis, A. M., McAllister, J. T., & Carroll, J. (2009). Reconstructing foveal pit morphology from optical coherence tomography imaging. *British Journal of Ophthalmology, 93*(9), 1223–1227.

Fulton, A. B., Albert, D. M., & Craft, J. L. (1978). Human albinism. Light and electron microscopy study. *Archives of Ophthalmology, 96*(2), 305–310.

Gregor, Z. (1978). The perifoveal vasculature in albinism. *British Journal of Ophthalmology, 62*, 554–557.

Guillery, R. W., Okoro, A. N., & Witkop, C. J. (1975). Abnormal central visual pathways in the brain of a human albino. *Brain Research, 96*, 373–377.

Harvey, P. S., King, R. A., & Summers, C. G. (2006). Spectrum of foveal development in albinism detected with optical coherence tomography. *Journal of the American Association for Pediatric Ophthalmology and Strabismus, 10*(3), 237–242.

Hendrickson, A. (2005). Organization of the adult primate fovea. In P. L. Penfold & J. M. Provis (Eds.), *Macular degeneration* (pp. 1–20). Heidelberg: Springer-Verlag.

Hendrickson, A., Djajadi, H., Erickson, A., & Possin, D. (2006). Development of the human retina in the absence of ganglion cells. *Experimental Eye Research, 83*, 920–931.

Hendrickson, A., Troilo, D., Possin, D., & Springer, A. (2006). Development of the neural retina and its vasculature in the marmoset monkey *Callithrix jacchus*. *Journal of Comparative Neurology, 497*, 270–286.

Hoang, Q. V., Linsenmeier, R. A., Chung, C. K., & Curcio, C. A. (2002). Photoreceptor inner segments in monkey and human retina: Mitochondrial density, optics, and regional variation. *Visual Neuroscience, 19*, 395–407.

Hoffmann, M. B., Tolhurst, D. J., Moore, A. T., & Morland, A. B. (2003). Organization of the visual cortex in human albinism. *Journal of Neuroscience, 23*, 8921–8930.

Ilia, M., & Jeffery, G. (1999). Retinal mitosis is regulated by DOPA a melanin precursor that may influence the time at which cells exit the cell cycle: Analysis of patterns of cell production in pigmented and albino retinae. *The Journal of Comparative Neurology, 405*, 394–405.

Ilia, M., & Jeffery, G. (2000). Retinal cell addition and rod production depend on early stages of ocular melanin synthesis. *The Journal of Comparative Neurology, 420*, 437–444.

Isenberg, S. J. (1986). Macular development in the premature infant. *American Journal of Ophthalmology, 101*, 74–80.

Jeffery, G. (1997). The albino retina: An abnormality that provides insight into normal retinal development. *Trends in Neuroscience, 20*(4), 165–169.

Kelly, J. P., & Weiss, A. H. (2006). Topographical retinal function in oculocutaneous albinism. *American Journal of Ophthalmology, 141*(6), 1156–1158.

King, R. A., Oetting, W. S., Summers, C. G., Creel, D. J., & Hearing, V. J. (2007). Abnormalities of pigmentation. In D. L. Rimoin, J. M. Connor, R. E. Pyeritz, & B. R. Korf (Eds.). *Emery and Rimoin's principles and practice of medical genetics* (Vol. 3, pp. 3380–3427). New York: Churchill Livingstone.

King, R. A., Pietsch, J., Fryer, J. P., Savage, S., Brott, M. J., Russell-Eggitt, I., et al. (2003). Tyrosinase gene mutations in oculocutaneous albinism 1 (OCA1): Definition of the phenotype. *Human Genetics, 113*(6), 502–513.

Kinnear, P. E., Jay, B., & Witkop, C. J. J. (1985). Albinism. *Survey of Ophthalmology, 30*, 75–101.

LaVail, J. H., Nixon, R. A., & Sidman, R. L. (1978). Genetic control of retinal ganglion cell projections. *Journal of Comparative Neurology, 182*, 399–422.

Lee, K. A., King, R. A., & Summers, C. G. (2001). Stereopsis in patients with albinism: Clinical correlates. *Journal of the American Association for Pediatric Ophthalmology and Strabismus, 5*(2), 98–104.

Li, K. Y., & Roorda, A. (2007). Automated identification of cone photoreceptors in adaptive optics retinal images. *Journal of the Optical Society of America A, 24*(5), 1358–1363.

Lopez, V. M., Decatur, C. L., Stamer, W. D., Lynch, R. M., & McKay, B. S. (2008). L-DOPA is an endogenous ligand for OA1. *Public Library of Science Biology, 6*(9), 1861–1869.

Maldonado, R. S., Izatt, J. A., Sarin, N., Wallace, D. K., Freedman, S., Cotten, C. M., & Toth, C. (2010). Optimizing hand-held spectral domain optical coherence tomography imaging for neonates, infants and children. *Investigative Ophthalmology & Visual Science* (Online first, MS IOVS.09-443).

Mann, I. (1950). *The development of the human retina*. New York: Grune & Stratton.

Marmor, M. F., Choi, S. S., Zawadzki, R. J., & Werner, J. S. (2008). Visual insignificance of the foveal pit: Reassessment of foveal hypoplasia as fovea plana. *Archives of Ophthalmology, 126*(7), 907–913.

Neveu, M. M., Von Dem Hagen, E., Morland, A. B., & Jeffery, G. (2008). The fovea regulates symmetrical development of the visual cortex. *Journal of Comparative Neurology, 506*, 791–800.

Nusinowitz, S., & Sarraf, D. (2008). Retinal function in X-linked ocular albinism (OA1). *Current Eye Research, 33*, 789–803.

Oetting, W. S., Summers, C. G., & King, R. A. (1994). Albinism and the associated ocular defects. *Metabolic, Pediatric, and Systemic Ophthalmology, 17*, 5–9.

Pallikaris, A., Williams, D. R., & Hofer, H. (2003). The reflectance of single cones in the living human eye. *Investigative Ophthalmology and Visual Science, 44*(10), 4580–4592.

Provis, J. M., Diaz, C. M., & Dreher, B. (1998). Ontogeny of the primate fovea: A central issue in retinal development. *Progress in Neurobiology, 54*, 549–581.

Pum, D., Ahnelt, P. K., & Grasl, M. (1990). Iso-orientation areas in the foveal cone mosaic. *Visual Neuroscience, 5*, 511–523.

Reis, R. A. M., Ventura, A. L. M., Kubrusly, R. C. C., de Mello, M. C. F., & de Mello, F. G. (2007). Dopaminergic signaling in the developing retina. *Brain Research Reviews, 54*, 181–188.

Rha, J., Schroeder, B., Godara, P., & Carroll, J. (2009). Variable optical activation of human cone photoreceptors visualized using short coherence light source. *Optics Letters, 34*(24), 3782–3784.

Rohrschneider, K. (2004). Determination of the location of the fovea on the fundus. *Investigative Ophthalmology & Visual Science, 45*, 3257–3258.

Sanderson, K. J., Guillery, R. W., & Shackleford, R. M. (1974). Congenitally abnormal visual pathways in mink (Mustela) vision with reduced retinal pigment. *Journal of Comparative Neurology, 154*, 225–248.

Scott, A. W., Farsiu, S., Enyedi, L. B., Wallace, D. K., & Toth, C. A. (2009). Imaging the infant retina with a hand-held spectral-domain optical coherence tomography device. *American Journal of Ophthalmology, 147*(2), 364–373.

Seo, J. H., Yu, Y. S., Kim, J. H., Choung, H. K., Heo, J. W., & Kim, S. J. (2007). Correlation of visual acuity with foveal hypoplasia grading by optical coherence tomography in albinism. *Ophthalmology, 114*(8), 1547–1551.

Springer, A. D. (1999). New role for the primate fovea: A retinal excavation determines photoreceptor deployment and shape. *Visual Neuroscience, 16*, 629–636.

Springer, A. D., & Hendrickson, A. E. (2004a). Development of the primate area of high acuity. 1. Use of finite element analysis models to identify mechanical variables affecting pit formation. *Visual Neuroscience, 21*, 53–62.

Springer, A. D., & Hendrickson, A. E. (2004b). Development of the primate area of high acuity. 2: Quantitative morphological changes associated with retinal and pars plana growth. *Visual Neuroscience, 21*, 775–790.

Springer, A. D., & Hendrickson, A. E. (2005). Development of the primate area of high acuity. 3: Temporal relationships between pit formation, retinal elongation and cone packing. *Visual Neuroscience, 22*(2), 171–185.

Summers, C. G. (1996). Vision in albinism. *Transactions of the American Ophthalmological Society, 94*, 1095–1155.

Summers, C. G. (2009). Albinism: Classification, clinical characteristics, and recent findings. *Optometry and Vision Science, 86*(6), 659–662.

Tanna, H., Dubis, A. M., Ayub, N., Tait, D. M., Rha, J., Stepien, K. E., & Carroll, J. (2009). Retinal imaging using commercial broadband optical coherence tomography. *British Journal of Ophthalmology*. doi:10.1136/bjo.2009.163501.

von dem Hagen, E. A. H., Houston, G. C., Hoffman, M. B., Jeffery, G., & Morland, A. B. (2005). Retinal abnormalities in human albinism translate into a reduction of grey matter in the occipital cortex. *European Journal of Neuroscience, 22*, 2475–2480.

von dem Hagen, E. A., Houston, G. C., Hoffmann, M. B., & Morland, A. B. (2007). Pigmentation predicts the shift in the line of decussation in humans with albinism. *The European Journal of Neuroscience, 25*(2), 503–511.

Wilson, H. R., Mets, M. B., Nagy, S. E., & Kressel, A. B. (1988). Albino spatial vision as an instance of arrested visual development. *Vision Research, 28*(9), 979–990.

Yuodelis, C., & Hendrickson, A. (1986). A qualitative and quantitative analysis of the human fovea during development. *Vision Research, 26*(6), 847–855.